Acoustic Excitation of Structures Analyzed by the Statistical Energy Method

J. J. Pocha*
Hawker Siddeley Dynamics Ltd., Stevenage, England

This paper presents the application of the Statistical Energy Method to the analysis of the acoustical response of spacecraft structures. The structures are assemblages of flat plates and cylinders interconnected in several ways. The analytic results were verified against a comprehensive test program in which representative structures were exposed to a reverberant sound field. In general, the correlation between test results and theoretical predictions was good, and indicates the manner in which the Statistical Energy Method can be used to obtain predictions in a relatively simple manner.

Nomenclature

A = surface area
C_a = speed of sound in air
E_1 = energy of system 1
M_1 = mass of system 1
n_1 = modal density of system 1
R_{rad} = radiation resistance of flat plate
R_{mech} = internal resistance (due to damping) of flat plate
$S_{a_1}(\omega)$ = power spectral density of normal acceleration of system 1
$S_{p_1}(\omega)$ = power spectral density of pressure of system 1
η_1 = loss factor of system 1 (due to dissipation)
η_{12} = coupling factor between systems 1 and 2
ρ = density
ω = circular frequency in rad/sec
ζ = damping coefficient

Subscripts‡

a = air
AF = acoustically fast modes
AS = acoustically slow modes
c = cylinder
f = floor
h = hoop (or circumferential stringer)
s = structure

Introduction

IN recent years a growing need has been identified for an analytic tool that can be used meaningfully by the spacecraft designer to obtain the response of structures to acoustic environments. Ideally, the tool should be easy to understand, easy and economical to use, and give realistic results of parameters meaningful to the design process. Furthermore, it should retain these properties for evaluations over the entire frequency range of interest. For the case of acoustic excitation, the frequency range could extend from the lowest natural frequencies of the structure to several kilohertz. The tool should be capable of being used at an early stage in spacecraft design to enable it to highlight possible areas, and should be economical enough so that it can be used freely to explore various solutions. Thorough analysis at an early stage in design can be the most cost-effective approach to spacecraft design. We describe here an attempt to satisfy such a requirement.

Presented at the AIAA/ASME/SAE 17th Structures, Structural Dynamics, and Materials Conference, King of Prussia, Pa., May 5-7, 1976 (in bound volume of Conference papers, no paper number); submitted June 8, 1976; revision received Oct. 25, 1976.

Index category: Structural Dynamic Analysis.

*Section Leader, Dynamics Dept., Space Division.

‡Numerical subscripts relate to systems and are described in the text as they occur.

Two basic methods are available; the classical modal method for low-frequency analysis, and the more recent statistical energy method for analysis in the high-frequency range. The first method produces good results only in the low-frequency range and for the lower modes of structure. The method is patently unsuitable for high-frequency work because of its demands of time and money.

This situation prompted the adoption of the statistical energy method, initially for very simple basic structures, and subsequently for complex structures. This method is not yet fully established in the armory of analytic techniques available to the designer, and yet it is capable of being used with good effect, producing realistic results with commendable economy of effort for certain problems not easily tractable by other means. It is hoped that this report of its successful use will encourage its application to suitable problems.

Application of the SEM to Spacecraft Structures

The principles underlying the statistical energy method are lucidly explained in Refs. 1-5 by the authors largely responsible for its early development. Here we shall proceed to consider the application of the method to spacecraft structures.

A large variety of spacecraft structures can be considered to be assemblages of flat plates and right cylinders interconnected into complex structures. It is therefore important to verify the method for the basic elements such as plates and cylinders before embarking on complex structures. This will also serve to highlight the simplicity of the method.

The response of a flat plate immersed in a reverberant acoustic field can be obtained from the energy balance equation of the plate. This reads: Power transferred from acoustic field to plate = Power dissipated by plate and can be written as

$$\omega n_2 \eta_{12}\left[\frac{E_1}{n_1} - \frac{E_2}{n_2}\right] = \omega \eta_2 E_2 \tag{1}$$

where system 1 refers to the acoustic field, and system 2 to the structure. Expressed in more commonly known parameters, this equation can be rewritten as

$$\frac{S_{a_2}(\omega)}{S_{p_1}(\omega)} = \frac{2\pi^2 n_2 C_a}{M_2 \rho_a}\left[\frac{R_{\text{rad}}}{R_{\text{rad}} + R_{\text{mech}}}\right] \tag{2}$$

A knowledge of the modal density of the plate, its damping, and the nature of the coupling between the acoustic field and the plate allows us to obtain the acceleration spectral density of the plate in terms of the excitation pressure spectral density

of the acoustic field. It can be seen that the response equation is very simple to evaluate. This simplicity masks, to some extent, the complexity of the analytic evaluation of the parameters such as modal density and radiation resistance. These are obtained on the basis of the overall vibration properties of the system in question. This is not the place to set out their full derivations; these can, however, be found in the literature on the subject. Particularly useful work has been done by the authors of Refs. 6-8.

Consider now the response of a cylinder immersed in a reverberant acoustic field. Here we encounter two mode groups for the cylinder itself, differentiated by their very different properties of coupling with the acoustic field. The first group is that of the acoustically slow modes, whose wave speeds are subsonic and which are therefore weakly coupled to the sound field. The second group is that of the acoustically fast modes whose wave speeds are supersonic, and which are consequently relatively strongly coupled to the sound field. A further mode group is that of the air cavity within the cylinder, and hence we have a vibration system comprising four interacting mode groups. The energy balance equations for the cylinder and internal air cavity mode groups can be written as

$$\omega\eta_{12AS}n_{2AS}\left[\frac{E_1}{n_1}-\frac{E_{2AS}}{n_{2AS}}\right]-\omega\eta_{23AS}n_{2AS}\left[\frac{E_{2AS}}{n_{2AS}}-\frac{E_3}{n_3}\right]=\omega\eta_2E_{2AS} \tag{3}$$

$$\omega\eta_{12AF}n_{2AF}\left[\frac{E_1}{n_1}-\frac{E_{2AF}}{n_{2AF}}\right]-\omega\eta_{23AF}n_{2AF}\left[\frac{E_{2AF}}{n_{2AF}}-\frac{E_3}{n_3}\right]=\omega\eta_2E_{2AF} \tag{4}$$

$$\omega\eta_{23AS}n_{2AS}\left[\frac{E_{2AS}}{n_{2AS}}-\frac{E_3}{n_3}\right]+\omega\eta_{23AF}n_{2AF}\left[\frac{E_{2AF}}{n_{2AF}}-\frac{E_3}{n_3}\right]=\omega\eta_3E_3 \tag{5}$$

where system 1 denotes the acoustic field, 2 denotes the cylinder mode groups, and 3 denotes the internal air cavity mode group. The remaining parameters are to be found in the Nomenclature.

From the previous equations, the response equations can be written as:

$$\frac{S_{a_2}(\omega)}{S_{p_1}(\omega)}=\frac{2\pi^2C_a}{A\rho_s\rho_a}\left[\frac{\eta_{21AF}n_{2AF}}{2\eta_{21AF}+\eta_2}+\frac{\eta_{21AS}n_{2AS}}{2\eta_{21AS}+\eta_2}\right]\times\left[1+\frac{S_{p_3}(\omega)}{S_{p_1}(\omega)}\right] \tag{6}$$

$$\frac{S_{p_1}(\omega)}{S_{p_3}(\omega)}=\frac{\eta_{21AS}n_{2AS}+\eta_{21AF}n_{2AF}+\eta_3n_3}{\dfrac{\eta_{2AS}^2n_{2AS}}{2\eta_{21AS}+\eta_2}+\dfrac{\eta_{21AF}^2n_{2AF}}{2\eta_{21AF}+\eta_2}}-1 \tag{7}$$

where it has been assumed that $\eta_{12}=\eta_{23}$ for both fast and slow mode groups, and that the energy of the cylinder is the sum of the fast and slow mode group energies. Once more, the individual parameters such as model densities and coupling factors must be obtained from an analysis of the vibratory characteristics of the structure (consult Refs. 7 and 8).

The basic flat plate and cylinder structures described above can be combined to form complex spacecraft-type structures as shown in Fig. 1. The statistical energy method can be used to analyze such structures by taking into account the energy transfer properties of the connections between two substructures, e.g., cylinder and flat plate or cylinder and stiffener. In the discussion below we shall evaluate the effect of

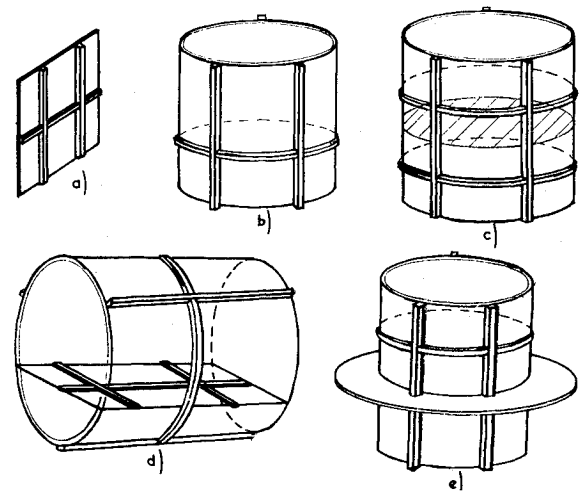

Fig. 1 Structures considered.

stiffeners (or stringers) on flat plates and cylinders, and the coupling mechanism between such structures.

We consider first the effect of stiffeners on a structure. Figure 1a shows a typical stiffened plate structure. It can be shown that the primary influence of a stiffener is to alter the radiation resistance below the coincidence frequency of the structure on which it is mounted. The radiation resistance of the acoustically slow modes is increased, owing to the scattering of the flexural waves impinging upon the stiffener. This leads to a higher coupling between the structure and the acoustic field, resulting in higher structure response. The physical mechanism whereby this is achieved is as follows: owing to the fact that the stiffener causes some distortion in the otherwise sinusoidal modal deflections of the structure, there is no longer volume velocity cancellation of the opposite sign phase cells adjacent to the stringer. Hence surface radiation is enhanced. In fact, the panel can be considered to be divided into subpanels by the stringers, and these subpanels then behave as would a panel without stringers. In the derivation of the slow mode radiation resistance of the structure, therefore, the radiating length is equal to the panel perimeter plus twice the total length of the stiffeners.

We now examine the nature of the coupling between two substructures and derive the related energy balance equations. Consider the structure such as shown in Fig. 1c, i.e. a cylinder with a transverse floor. The coupling between the cylinder and floor (connected to the cylinder along its periphery) can be considered to be strong, in the sense that the coupling coefficient is considerably greater than the dissipation coefficient (due to material damping) of the structure.

This enables us to invoke the principle of equipartition of energy which states that, for two strongly coupled interacting systems, the energy of each mode of each system is equal to the energy of every other mode.

This is not to say that the energy content of the two structures is the same, as the energy is a function of the modal density, and the structure with the higher modal density will have the greater energy. This allows us to write

$$E_c/E_f=n_c/n_f \tag{8}$$

We can now state the energy balance relations for the cylinder and flpor. In the equations that follow, the parameters will be designated by suffixes relating to the components as: Suffix 1 = reverberant acoustic field, Suffix 2 = cylinder skin, further subdivided into AF (fast) as AS (slow) modes, Suffix 3 = internal air cavity, and Suffix 4 = internal floor. The energy balance equation for the cylinder skin can be written as: Power transmitted to skin = power dissipated by skin + power transmitted to air cavity + power transmitted to floor.

According to our symbology this, for the acoustically fast modes, can be written

$$\omega\eta_{21AF}n_{2AF}\left[\frac{E_1}{n_1}-\frac{E_{2AF}}{n_{2AF}}\right]-\omega\eta_{23AF}n_{2AF}\left[\frac{E_{2AF}}{n_{2AF}}-\frac{E_3}{n_3}\right]$$

$$-\omega\eta_2E_{2AF}-\omega E_4^I\eta_4=0 \tag{9}$$

and a similar equation applies for the slow modes. The term $(\omega E_4^I\eta_4)$ requires explanation. It is the energy the floor obtains due to energy transmission of the cylinder fast modes. This energy transmission is obtained from the relationship for the floor

Power transmitted to floor = Power dissipated by floor

$$=\omega\eta_4E_4^I$$

Now consider the last two terms of Eq. (1), i.e.,

$$-(\omega\eta_2E_{2AF}+\omega\eta_4E_4^I)$$

The principle of equipartition of energy applied to cylinder-floor coupling gives the following relationships for the fast and slow mode groups

$$\frac{E_4^I}{E_{2AF}}=\frac{n_4}{n_{2AF}}\quad\text{and}\quad\frac{E_4^{II}}{E_{2AS}}=\frac{n_4}{n_{2AS}} \tag{10}$$

Substituting E_4^I from Eq. (3) into Eq. (2) gives

$$=-(\omega\eta_2E_{2AF}+\omega\eta_4(n_4/n_{2AF})E_{2AF})=\omega\eta_2^IE_{2AF}$$

where

$$\eta_2^I=\eta_2+(n_4/n_{2AF})\eta_4 \tag{11}$$

Hence the effect of the floor is effectively to increase the damping of the cylinder. In terms of system energies, this is an eminently sensible concept, as the floor provides an additional loss path for the energy incident upon the cylinder.

We can now write the response equation in terms of useful parameters as

$$\frac{S_{a_2}(\omega)}{S_{p_1}(\omega)}=\frac{2\pi^2C_a}{A_{psp\alpha}}\left[\frac{\eta_{21AF}n_{2AF}}{2\eta_{21AF}+\eta_2^I}+\frac{\eta_{21AS}n_{2AS}}{2\eta_{21AS}+\eta_2^{II}}\right]\times\left[1+\frac{S_{p_3}(\omega)}{S_{p_1}(\omega)}\right] \tag{12}$$

$$\frac{S_{p_1}(\omega)}{S_{p_3}(\omega)}=\frac{\eta_{21AF}n_{2AF}+\eta_{21AS}n_{2AS}+\eta_3n_3}{\dfrac{\eta_{21AF}^2n_{2AF}}{2\eta_{21AF}+\eta_2^I}+\dfrac{\eta_{21AS}^2n_{2AS}}{2\eta_{21AS}+\eta_2^{II}}}-1 \tag{13}$$

$$\frac{S_{a_2}(\omega)}{S_{a_4}(\omega)}=\frac{M_4n_2}{M_2n_4} \tag{14}$$

If there are stiffeners on the skin and/or on the floor, their response is obtained by equipartition of energy with the substructure to which they are attached.

Structures such as shown in Fig. 1e are considered in the following manner: here we have the case that both substructures, the floor and the cylinder, are excited by the reverberant field, and their energy balance equations can be written as: For the cyclinder

Energy input to cylinder = energy dissipated by cylinder

+ energy transmitted to air cavity

± energy transmitted to floor

For the floor

Energy input to floor = energy dissipated by floor

+ energy gained from the cylinder

The energy transfer between the floor and the cylinder depends upon the difference between their modal energies. Since both substructures are exposed to the acoustic field, they will both receive energy from that field, and their modal energies will be comparable. This will result in the energy transfer between the floor and the skin being low, in any case, very low in comparison with the energy received from the acoustic field. In the energy balance formulation, therefore, the interstructure energy transfer terms are neglected. This has the effect of decoupling the two substructures, except that the effect of the floor on the skin is now that of a circumferential stiffener.

Having decoupled the structure, the response of the component parts can be obtained separately for the flat plate and cylinder with internal air cavity.

Experimental Program

In order to derive confidence in the analytic techniques and in the assumptions underlying the response equations formulated above, a comprehensive test program was undertaken. Five basic structures were tested, these being: 1) flat plate, 2) right cylinder, 3) cylinder with transverse internal floor, 4) cylinder with longitudinal internal floor, 5) cylinder with transverse external floor.

These structures were instrumented with accelerometers, mounted in a reverberation chamber from low-frequency supports (to simulate free-free boundary conditions), and subjected to a Thor-Delta type acoustic environment. The measured response was then compared with theoretical predictions.

The tests were carried out in the Ling RCH-192 reverberation chamber at ESTEC, Holland. The chamber internal volume is 192 ft^3, and it is driven by twin sirens that feed air into the chamber through an exponential horn. The sirens are driven by either an ASDE 80 random noise generator or a B and K 1013 sine wave generator. The frequency range of the chamber extends from about 50 Hz to 20,000 Hz, though above 10,000 Hz the available sound energy is very low. The maximum mean sound pressure level achievable is 163 dB relative to a pressure of a $2\times10^{-5}N/m^2$. Figure 2 is a diagrammatic representation of the acoustic chamber and associated instrumentation.

The test structures were sized with two requirements in mind. First, they should fit within the working volume of the chamber, which can be taken to be approximately 1/10th the chamber volume around the center point of the chamber. Second, they should be such as to enable us to investigate all the vibration regimes of the structures. This implies that the material properties, thickness, etc. should be such that the coincidence frequency is around 5 kHz to 6 kHz, and the cylinder ring frequency around 2 kHz to 3 kHz. In fact, the structures were such that the coincidence frequency was 5660

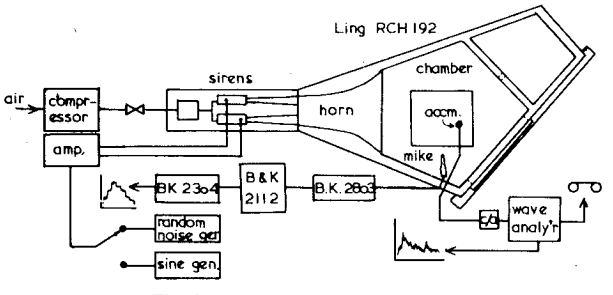

Fig. 2 Acoustic chamber facility.

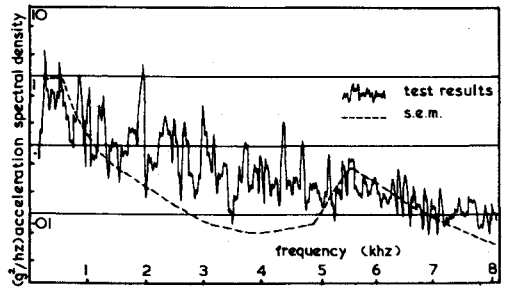

Fig. 3 Flate plate response.

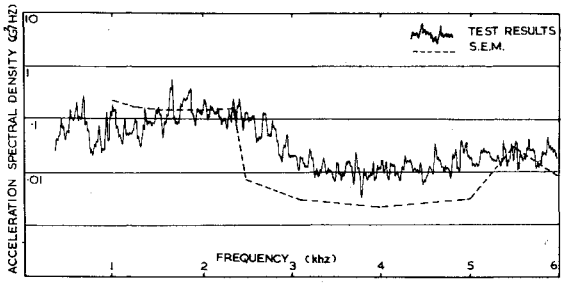

Fig. 4 Cylinder response.

Hz in all cases, and the ring frequency 2430 Hz for structures 1b, 1c and 1d, and 4255 Hz for structure 1e. The structures were fabricated of aluminium 2 mm in thickness and interstructure connections were obtained by continuous or near-continuous welding. The test program is described in detail in Refs. 9 and 10.

Comparison Between Test Results and Theory

We shall discuss the correlation between test results and theoretical predictions for each of the structures in turn. For the theoretical predictions, an empirically derived material damping factor (i.e the ratio between damping and critical damping) of 1% (or 0.01) has been used for structures 1a and 1b, and a value of 0.5% (or 0.005) for structures 1c, 1d and 1e. These values are thought to be representative of the type of structure, material, and construction considered here.

Flat Plate

The comparison between test results and theory is shown for a typical accelerometer output in the frequency range of 0 to 6 kHz (see Fig. 3). It is to be noted that theory gives the space-averaged response for the plate. In the 0 to 2 kHz range agreement between the two is seen to be rather good. For the larger frequency range, the agreement above the coincidence frequency – 5660 Hz – is seen to be very good, while below it, i.e. is the 2 to 5 kHz range the theory underestimates the response. To some extent, this is due to the rather artificial division between the fast and slow mode regimes assumed by the theory. In practice, the coupling between the field and the plate will vary rather more gradually, resulting in a higher response below the coincidence frequency.

Circular Cylinder

The comparison between test results and theory is shown in Fig. 4 for a typical accelerometer in the range of 0 to 6 kHz. In the theoretical plot, three distinct radiation regimes are evident. Below 2430 Hz (the ring frequency) both fast and slow modes exist, and the radiation, and therefore the response is governed by the fast modes. In this regime, agreement between theory and experiment is seen to be good. Between the ring and coincidence frequencies only slow modes can exist and hence the response exhibits a distinct trough. Here agreement between theory and experiment is not good, mainly for the reasons outlined previously. Above the

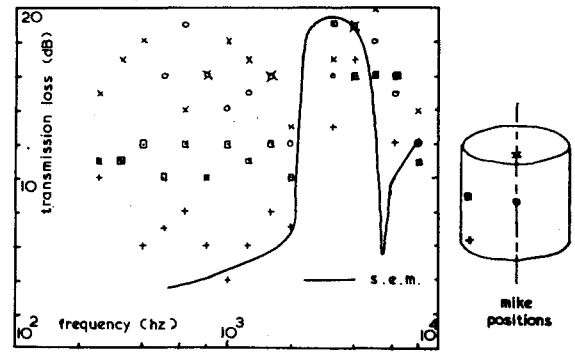

Fig. 5 Cylinder transmission loss.

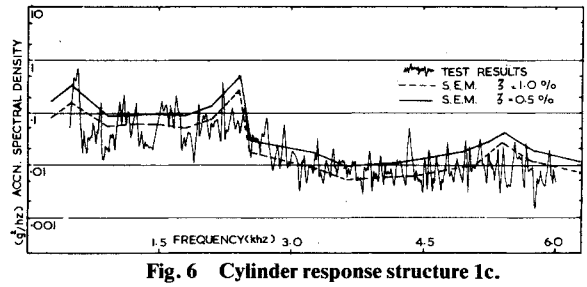

Fig. 6 Cylinder response structure 1c.

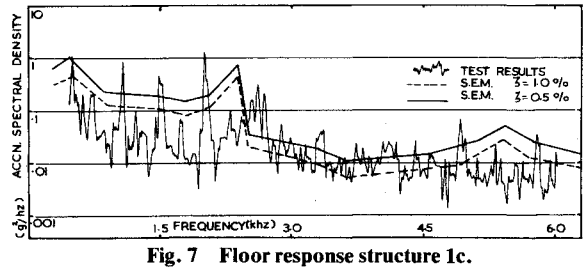

Fig. 7 Floor response structure 1c.

coincidence frequency, only fast mode radiation occurs and agreement between theory and experiment is, once more, good.

Comparison between measured and predicted transmission loss is shown in Fig. 5. A large variation with internal microphone position is apparent. Considering each regime in turn, we see that below the ring frequency, the theory agrees best with the results of the microphone mounted close to the wall and one end-cap. Worst agreement is obtained for the positions along the cylinder axis. This behavior is consistent with the argument that some pressure wave cancellation at a position of geometric symmetry is to be expected. This would result in lower pressures along the cylinder axis and consequently higher values of transmission loss. The same argument would also confirm that the theoretical prediction is the lower bound.

In the frequency regime between the ring and coincidence frequencies, we have already seen that theory underestimates the structure response. Since the internal cavity is energized directly by the structure, we would expect the theory to yield low internal pressure and therefore a high transmission loss in this regime. This is consistent with the results obtained. The results in the regime above coincidence can be explained by the same argument as was used for the regime below the ring frequency. The lower scatter is probably due to the less exact pressure cancellation at high frequencies, and to the fact that in this regime radiation is due solely to the fast modes, and is therefore relatively well ordered.

Circular Cylinder with Transverse Floor

This was the first complex structure tested, and included longitudinal stiffeners on the cylinder skin and a transverse

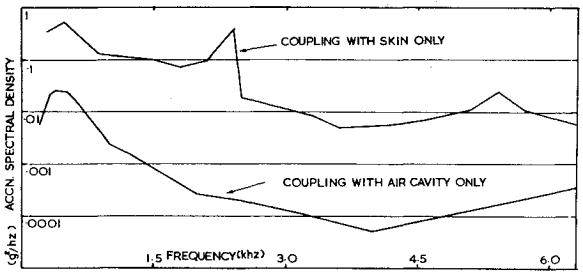

Fig. 8 Floor response structure 1c.

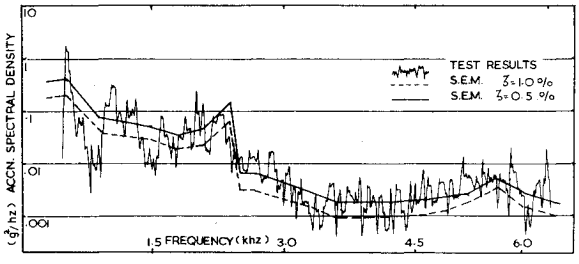

Fig. 9 Cylinder stringer response structure 1c.

floor (see Fig. 1c). We shall discuss the agreement between theory and experiment for each substructure in turn. Considering the cylinder first, a typical plot is shown in Fig. 6. Agreement is seen to be quite good above 1500 Hz. The theoretical prediction, which is the space average, showed good agreement with the individual accelerometer responses.

Agreement is better for the 0.5% damping case than for the 1% case. This will be seen to be the case for all the structures and substructures considered. On comparing the full range (0 to 6 kHz) rms values measured and predicted we see that the theory underestimates the response. Examination of the spectra indicates that this is due to the energy within strongly excited individual modes in the low-frequency regime. Under these conditions, the statistical energy method is not properly applicable and discrepancies must result. To verify this hypothesis, the rms values of the measured response was obtained within two separate bandwidths 100 Hz to 6 kHz, and 2700 Hz to 6 kHz. The latter gives the rms value of the energy within the high-frequency regime only, where theory can be expected to yield good results. Table 1 indicates that this is indeed the case.

We now consider the internal floor. A typical plot is shown in Fig. 7. It indicates good agreement over almost the entire frequency range, especially for a value of damping factor of 0.5%. Agreement between theory and space-averaged test results is also close. Comparison of rms values shows that reasonably good agreement is obtained for the high-frequency regime, 2700 Hz to 6000 Hz, (see Table 1). The theoretical derivation of the response of the internal floors has considered the floor to receive its energy solely through its coupling with the cylinder.

In fact there is an additional energy transfer path – that between the floor and the internal air cavities. In theory, this is assumed to be negligible because the energy in the internal air cavity is very low compared to that of the outside field, and because the coupling between the floor and air cavities is considerably weaker than that between the floor and the skin. To test this hypothesis we obtained the response of the floor due to the coupling with the cylinder only, and with the coupling of the air cavities only. The results are shown in Fig. 8. It can be seen that the floor response due to coupling with the cylinder is considerably greater than that due to coupling with the air cavity. The results for the floor show that the theoretical assumptions are reasonable, i.e. the floor and cylinder can be considered to be strongly coupled, and the principle of equipartition of energy therefore applies.

Comparison between theory and experiment for the cylinder axial stiffeners is shown in Fig. 9. The theoretical prediction using a damping factor of 0.5% is seen to give good agreement with test results over the whole frequency range. Evaluation of the rms values reinforces this observation, as shown in Table 1. The behavior of the internal air cavities is as before.

Circular Cylinder with Longitudinal Floor

The structures has a longitudinal floor displaced a certain distance from the axis of the cylinder (Fig. 1d). The cylinder

Table 1 Structure 1c rms values in G

Structure	No. of Accms.	Measured space Averaged resp.		Theoretical predictions $\zeta=1.0\%$		$\zeta=0.5\%$	
		0.1-6 kHz	2.7-6 kHz	0.1-6 kHz	2.7-6 kHz	0.1-6 kHz	2.7-6 kHz
Cylinder	4	29	11	16	5.7	22	7.8
Floor	6	47	9.4	22	5.7	29	7.8
Stringers	2	24	5.8	12	2.2	16	3

Table 2 Structure 1d rms values in G

Structure	No. of Accms.	Measured space Averaged resp.		Theoretical predictions $\zeta=1.0\%$		$\zeta=0.5\%$	
		0.1-6 kHz	2.7-6 kHz	0.1-6 kHz	2.7-6 kHz	0.1-6 kHz	2.7-6 kHz
Cylinder	6	26.7	8.3	11	4	16	5.4
Floor	4	26	6.2	16	4	22.5	5.4
Cylinder Stringer	1	16.5	3.3	9.7	1.5	12.7	2.0
Cylinder Hoop	1	23.6	5.3	16.5	2.5	22	3.4
Floor Stringers	2	12.7	2.46	9.7	1.5	12.7	2.0

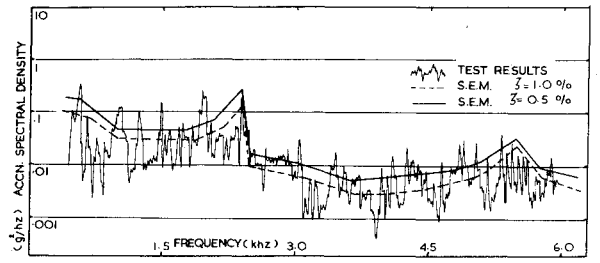

Fig. 10 Cylinder response structure 1d.

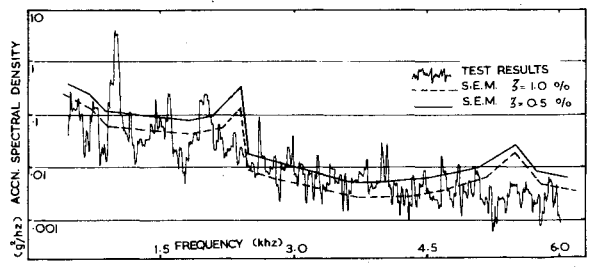

Fig. 11 Floor response structure 1d.

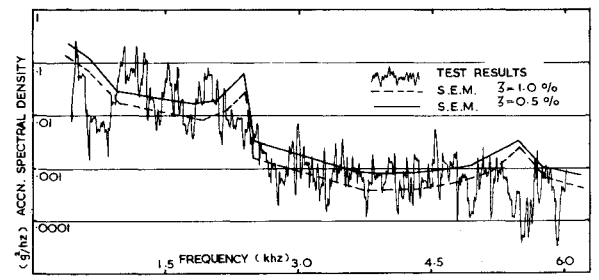

Fig. 12 Cylinder stringer response structure 1d.

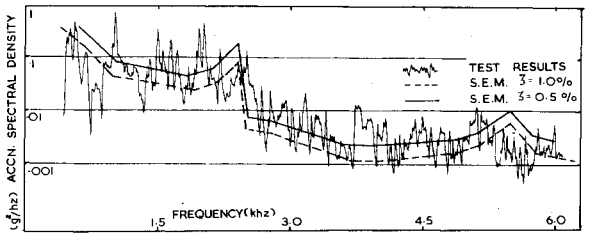

Fig. 13 Cylinder hoop response structure 1d.

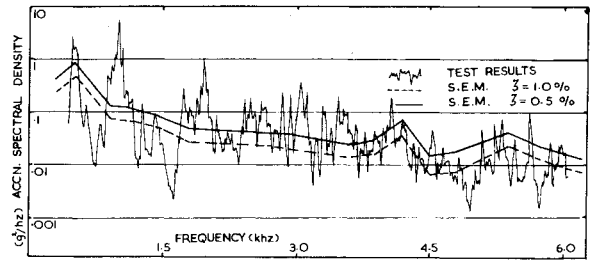

Fig. 14 Cylinder response structure 1e.

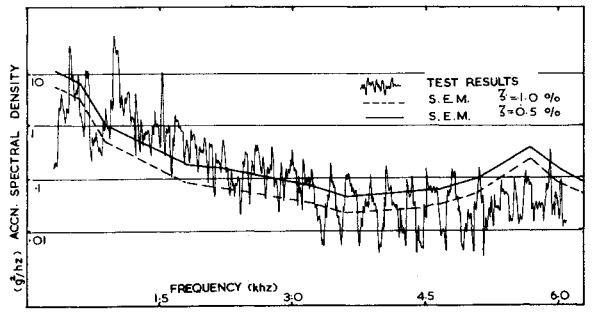

Fig. 15 Floor response structure 1e.

has axial and circumferential stiffeners, and there are stiffeners on the floor.

The comparison between theory and experiment for the cylinder is shown in Fig. 10. A damping factor of 0.5% yields good agreement over almost the full frequency range, with better agreement being obtained at the high frequencies. Good agreement is also obtained for the space-averaged test results. Comparing now the rms values shown in Table 2, it is seen that the full range values do not conform to expectations. This, again, is primarily due to energy concentration in individual low-frequency modes. Better agreement is obtained when the rms values of the high-frequency regime (2700 to 6000 Hz) are compared.

The floor response is shown in Fig. 11. Once again, good agreement is obtained over a wide frequency range, especially for the case of 0.5% damping. As can be expected, agreement with the space-average test results is also good. Comparison between the measured and predicted rms values, shown in Table 2, indicates good agreement, especially in the high-frequency regime (2700 to 6000 Hz).

The results of the cylinder stiffeners, axial and circumferential, are shown in Figs. 12 and 13, respectively. The theory is seen to agree very well with test results over almost the entire frequency range, when the damping factor is taken to be 0.5%. The rms values, shown in Table 2, indicate good agreement for both the full range and the high-frequency range. The same comments apply for the floor stiffeners. The behavior of the internal air cavities is as before.

Circular Cylinder with External Transverse Floor

The structure is illustrated in Fig. 1e and is seen to have a transverse external annular floor and axial cylinder stiffeners. The cylinder response shown in Fig. 14 exhibits reasonably good agreement over most of the frequency range. The theory cannot predict the concentrations of energy in individual modes at the low-frequency end of the spectrum, but the overall agreement is reasonably good, and better for a damping factor of 0.5%. Comparison between the rms values is shown in Table 3, and reflects the behavior of the spectra in that the values predicted by theory are significantly lower than measured values. It is seen that above about 3500 Hz, when the modal density is reasonably high and a number of fast modes occur, the agreement between theory and test results is quite good.

Table 3 Structure 1e rms values in G

Structures	No. of Accms.	Measured space Averaged resp.		Theoretical predictions $\zeta = 1.0\%$		$\zeta = 0.5\%$	
		0.1-6 kHz	2.7-6 kHz	0.1-6 kHz	2.7-6 kHz	0.1-6 kHz	2.7-6 kHz
Cylinder	5	40	17.54	16	7.2	21	9.5
Floor	5	140	19.4	51	14.1	71	18.4
Stringers	2	36	6.31	18	3.4	23	4.4

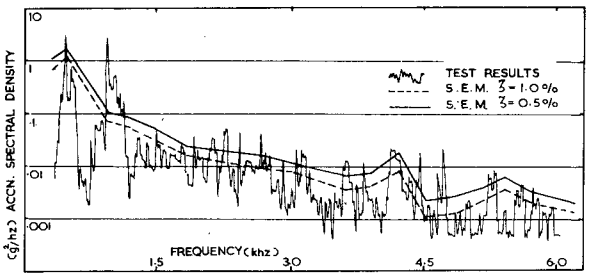

Fig. 16 Cylinder stringer response structure 1e.

A typical result for the external floor response is shown in Fig. 15. It is seen that the response is considerably higher than for any other structure compoment, and the bulk of the energy is concentrated within the low-frequency regime. The comparison between theory and experiment is reasonably good, except at low frequencies. Comparison of the rms values naturally highlights this behavior, poor agreement being obtained for the full-range values and good agreement being obtained for the high-frequency regime (2700 Hz to 6000 Hz).

Figure 16 shows the comparison between theory and experiment for the axial cylinder stiffeners. Good agreement is obtained over almost the entire frequency range, especially for a damping factor of 0.5%. The theory and the measured 1/3 octave space-averaged response are also in good agreement. The rms values reflect the behavior of the spectra, and good agreement is obtained. The internal air cavity response is once again as before.

Conclusions

For the structures considered, the overall agreement between theory and experiment is seen to be reasonably good. The response prediction for the individual structure components is seen to be in good agreement with test results over a wide frequency range. This agreement indicates that the theory is capable of describing the physical mechanisms involved in the acoustic excitation process with a good degree of realism. In particular, it is seen that the assumption of strong interstructure coupling is well borne out and yields good results. Such coupling allows us to invoke the principle of equipartition of modal energy, and considerably simplifies the analysis of the system. In fact, one of the highlights of the method is the analytic simplicity of the solution. When programed for the digital computer, the method is very easy to use, cheap to run, and provides reliable and realistic results. The method has considerable potential and should be developed further to account for more complex systems.

Acknowledgment

This work was supported by the European Space Agency.

References

[1]Smith, P.W. Jr., and Lyon, R.H., "Sound and Structural Vibration," NASA CR-160, March 1965.

[2]Lyon, R. H., and Maidanik, G., "Power Flow between Linearly Coupled Oscillators," *The Journal of the Acoustical Society of America*, Vol. 34, May 1962, pp. 623-639.

[3]Ungar, E. E., "Fundamentals of Statistical Energy Analysis," Air Force Flight Dynamics Laboratory, Wright-Patterson AFB, Ohio, Rept. AFFDL-TR-66-5.2, May 1966.

[4]Lyon, R. H., "Statistical Energy Analysis of Dynamical Systems: Theory and Applications," MIT Press, Cambridge, Mass 1975.

[5]Dyer, I., "Moment Impedance of Plates," *Journal of the Acoustical Society of America*, Vol. 32, Oct. 1960, pp. 1290-1297.

[6]Maidanik, G., "Response of Ribbed Panels to Reverberant Acoustic Fields," *Journal of the Acoustical Society of America*, Vol. 34, June 1962, pp. 809-826.

[7]Manning, J. E. and Maidanik, G., "Radiation Properties of Cylindrical Shells," *The Journal of the Acoustical Society of America*, Vol. 36, Sept. 1964, pp. 1691-1698.

[8]Hart, F.D. and Shah, K.C., "Compendium of Modal Densities of Structures," NASA CR-1773, July 1971.

[9]Pocha, J. J., "The Acoustic Excitation of Structures: Final Report, Vol. 1," European Space Agency, CR-596, June 1975.

[10]Pocha, J. J., "The Acoustic Excitation of Structures: Phase 2 Final Report, Vol. 1," European Space Agency CR(P)-733, July 1975.